European Journal of Pharmacology 698 (2013) 413–420

Contents lists available at SciVerse ScienceDirect

European Journal of Pharmacology

journal homepage: www.elsevier.com/locate/ejphar

Immunopharmacology and inflammation

The role of PKC/ERK1/2 signaling in the anti-inflammatory effect of tetracyclic triterpene euphol on TPA-induced skin inflammation in mice

Giselle F. Passos [a], Rodrigo Medeiros [a], Rodrigo Marcon [a], Andrey F.Z. Nascimento [a], João B. Calixto [a,*], Luiz F. Pianowski [b]

[a] Department of Pharmacology, Universidade Federal de Santa Catarina, 88040-900, Florianópolis, Santa Catarina, Brazil
[b] Pianowski & Pianowski Ltda. Rua Coronel Luiz Leme, 400, 12914-010, Bragança Paulista, SP, Brazil

ARTICLE INFO

Article history:
Received 26 April 2012
Received in revised form
4 October 2012
Accepted 13 October 2012
Available online 23 October 2012

Keywords:
Euphol
TPA
Inflammation
PKC
MAPK
COX-2

ABSTRACT

Inflammation underlies the development and progression of a number of skin disorders including psoriasis, atopic dermatitis and cancer. Therefore, novel antiinflammatory agents are of great clinical interest for prevention and treatment of these conditions. Herein, we demonstrated the underlying molecular mechanisms of the antiinflammatory activity of euphol, a tetracyclic triterpene isolated from the sap of *Euphorbia tirucalli*, in skin inflammation induced by 12-O-tetradecanoylphorbol-13-acetate (TPA) in mice. Topical application of euphol (100 μg/ear) significantly inhibited TPA-induced ear edema and leukocyte influx through the reduction of keratinocyte-derived chemokine (CXCL1/KC) and macrophage inflammatory protein (MIP)-2 levels. At the intracellular level, euphol reduced TPA-induced extracellular signal-regulated protein kinase (ERK) activation and cyclooxygenase-2 (COX-2) upregulation. These effects were associated with euphol's ability to prevent TPA-induced protein kinase C (PKC) activation, namely PKCα and PKCδ isozymes. Our data indicate that topical application of euphol markedly inhibits the inflammatory response induced by TPA. Thus, euphol represents a promising agent for the management of skin diseases with an inflammatory component.

1. Introduction

The skin is the primary interface between the body and the environment, therefore, it is a major target for injury by a wide spectrum of physical, chemical and microbial agents that are capable of changing its structure and function (Bickers and Athar, 2006). These insults are usually translated into inflammation, a reaction required for successful cutaneous immune surveillance (Robert and Kupper, 1999). Although protective, inflammation may be associated with a number of skin disorders including psoriasis, atopic dermatitis, and cancer (Johnson-Huang et al., 2009; Mueller, 2006). The inflammatory process is characterized by the release of a number of mediators, including cytokines, chemotactic molecules, prostaglandins, and vasoactive peptides, which culminates in changes in vascular permeability and cellular infiltration (Levy, 1996). Extensive experimental evidence has shown that exposure of skin to 12-O-tetradecanoylphorbol-13-acetate (TPA) induces a pleiotrophic tissue response encompassing a strong inflammatory reaction similar to that observed in several skin diseases, and is one of the most potent and frequently used tumor promoters (Hvid et al., 2008; Verma et al., 2006). TPA stimulates the activation of a wide variety of intracellular pathways through the activation of protein kinase C (PKC), including mitogen-activated protein kinases (MAPKs) and nuclear factor-κB (NF-κB), as well as the generation of mediators like tumor necrosis factor (TNF)-α, interleukin (IL)-1β, keratinocyte-derived chemokine (CXCL1/KC), macrophage inflammatory protein (MIP)-2, and prostaglandins, among others (Cataisson et al., 2005,2006; Medeiros et al., 2007; Otuki et al., 2005).

Euphorbia tirucalli L. (Euphorbiaceae), commonly known as aveloz or pencil tree, is a subtropical and tropical ornamental plant, which is used in folk medicine for the treatment of several kinds of cancer, including basal cell carcinomas, leukemia, prostate and breast cancers (De Melo et al., 2011; Valadares et al., 2006). It has been demonstrated that the ethanolic extract of *E. tirucalli* significantly increases survival and reduces tumor growth in the peritoneal cavity of mice in the Ehrlich ascites carcinoma model (Valadares et al., 2006). One of the main constituents of the latex extracted from the plant is the tetracyclic triterpene euphol. Euphol isolated from the roots of *Euphorbia kansui* was shown to inhibit TPA-induced ear edema, as well as tumor-promotion in the two-stage carcinogenesis induced by 7,12-dimethylbenz[a]anthracene (DMBA)-TPA protocol in mouse skin (Yasukawa et al., 2000). However, the mechanisms underlying these effects remain to be elucidated.

Herein, we analyzed some of the molecular mechanisms through which euphol exerts its antiinflammatory action on TPA-induced skin responses in mice. Data presented indicate that

* Correspondence to: Departamento de Farmacologia, Universidade Federal de Santa Catarina, Campus Universitário, Trindade, Bloco D, CCB, Caixa Postal 476, CEP 88049-900, Florianópolis, SC, Brazil.
Tel.: +55 48 3721 9491x9764
E-mail addresses: calixto@farmaco.ufsc.br, calixto3@terra.com.br (J.B. Calixto).

0014-2999
http://dx.doi.org/10.1016/j.ejphar.2012.10.019

topical treatment with euphol isolated from *E. tirucalli* resulted in a consistent decline of TPA-induced skin inflammation as assessed by skin edema and leukocyte infiltration. Likewise, we observed an inhibitory effect of euphol on the activation of downstream signaling proteins, namely PKC and MAPKs, which in turn decreased the levels of CXC chemokines and cyclooxygenase-2 (COX-2) following topical application of TPA.

2. Materials and methods

2.1. Drugs and reagents

The following reagents were used: 12-O-tetradecanoylphorbol-13-acetate (TPA), 4-(2-Hydroxyethyl)piperazine-1-ethanesulfonic acid (HEPES), phosphate buffered saline (PBS), trisodium citrate, hydrogen peroxide, hematoxylin, $MgCl_2$, KCl, NaCl, NaH_2PO_4, Na_2HPO_4, phenylmethylsulphonyl fluoride, ethylenediaminetetraacetic acid (EDTA), paraformaldehyde, trypsin inhibitor, leupeptin, pepstatin A, aprotinin, sodium orthovanadate, β-glycerophosphate, sodium fluoride, dithiothreitol, hexadecyl trimethyl ammonium bromide, tetramethylbenzidine, 4-nitrophenyl N-acetyl-β-D-glucosaminide, Trizma base, Triton X-100, Tween 20, benzethonium chloride (Sigma-Aldrich, São Paulo, SP, Brazil), xylene, methanol, acetone, ethanol, HCl (Merck & Co., Inc., Whitehouse Station, NJ, USA), anti-p38, anti-extracellular signal-regulated protein kinase (ERK), anti-PKCα, anti-PKCε, anti-PKCδ (Santa Cruz Biotech. Inc., Santa Cruz, CA, USA), anti-phosphorylated (p)-p38 (Thr^{180} and Tyr^{182}), anti-p-ERK (Thr^{183} and Tyr^{185}) (Promega, Madison, WI, USA), anti-COX-2, and 3,3′-diaminobenzidine (DAB) (Dako, Glostrup, Denmark).

The tetracyclic triterpene euphol was extracted from the sap of *E. tirucalli* as previously described (Dutra et al., 2012). The purity of the obtained compound was $>98\%$.

2.2. Animals

Experiments were conducted using 8-week-old male Swiss CD-1 mice kept in a controlled room temperature (22 ± 2 °C) and humidity (50–60%) under a 12 h light/dark cycle (lights on 6:00 A.M.). All procedures used in the present study followed the "Principles of Laboratory Animal Care" from National Institutes of Health (NIH) publication number 85-23 and were approved by the Animal Ethics Committee of the Universidade Federal de Santa Catarina.

2.3. TPA-induced skin inflammation and ear edema measurement

Skin inflammation was induced in the right ear by the topical application of 2.5 μg/ear of TPA dissolved in 20 μl of acetone. Control animals received the same volume of acetone (vehicle) in the right ear. The ear edema was assessed at 2, 4, 6, 12 and 24 h after TPA application and was expressed as the increase in ear thickness due to the inflammatory challenge. Ear thickness was measured before and after induction of the inflammatory response by using a micrometer (Mitutoyo, Suzano, SP, Brazil) that was applied near the tip of the ear just distal to the cartilaginous ridges and the thickness was recorded in micrometer (μm). To minimize variation due to technique, a single investigator performed the measurements throughout any one experiment.

To evaluate the effect of euphol on TPA-induced skin inflammation, animals were topically treated with euphol (50–100 μg/ear) in conjunction with TPA. Control animals were treated with vehicle (acetone/ethanol, 3:1).

2.4. Myeloperoxidase and N-acetylglucosaminidase assays

Neutrophil and macrophage infiltration into the ear tissue was assessed indirectly by measuring myeloperoxidase (MPO) and N-acetylglucosaminidase (NAG) activities, respectively. The measurements were carried out in 6 mm punch-biopsies obtained from the mice ear 24 h after TPA-induced skin inflammation. Tissues were homogenized at 5% (w/v) in EDTA/NaCl buffer (pH 4.7) and centrifuged at 10,000*g* for 15 min at 4 °C. The pellet was resuspended in 0.5% hexadecyl trimethyl ammonium bromide buffer (pH 5.4), and the samples were frozen in liquid nitrogen and thawed three times. Upon thawing, the samples were centrifuged as above, and 25 μl of the supernatant was used for the MPO and NAG assays. The MPO enzymatic reaction was assessed by addition of 1.6 mM tetramethylbenzidine, 80 mM $NaPO_4$, and 0.3 mM hydrogen peroxide. NAG activity measurement was determined by adding 2.25 mM 4-nitrophenyl N-acetyl-β-D-glucosaminide and 100 μl 50 mM citrate buffer (pH 4.5). Absorbance was measured spectrophotometrically at 690 and 405 nm for MPO and NAG, respectively, and the results are expressed as optical density (OD)/mg tissue.

2.5. Western blot

The western blot analyses were carried out in 6 mm punch-biopsies obtained from the mice ear 2 h after TPA-induced skin inflammation. Tissues were homogenized in ice-cold lysis buffer [10 mM HEPES (pH 7.4), containing 1.5 mM $MgCl_2$, 10 mM KCl, 1 mM phenylmethylsulphonyl fluoride, 5 μg/ml leupeptin, 7 μg/ml pepstatin A, 10 μg/ml aprotinin, 1.5 μg/ml trypsin inhibitor, 2 mM sodium orthovanadate, 10 mM β-glycerophosphate, 50 mM sodium fluoride, and 0.5 mM dithiothreitol]. The homogenates were chilled on ice for 15 min and then centrifuged at 12,000*g* for 60 min at 4 °C. The supernatant containing the cytosolic fraction was collected and stored at −70 °C. The pellet was resuspended in lysis buffer containing 1% Triton X-100, homogenized and centrifuged at 12,000*g* for 30 min at 4 °C, and the supernatant containing the membrane fraction was stored at −70 °C. Protein concentration was determined using the protein assay kit according to the manufacturer's instructions (Bio-Rad, São Paulo, SP, Brazil).

Equal protein amounts were separated on a sodium dodecyl sulfate-polyacrylamide gel electrophoresis (SDS-PAGE), and then transferred to a polyvynilidene fluoride membrane (Immobilon P; Millipore, Bedford, MA, USA). The membranes were blocked by incubation with 10% non-fat dry milk solution and then incubated overnight with antibodies against p38 (dilution 1:1000), ERK (dilution 1:2000), (p)-p38 (Thr^{180} and Tyr^{182}) (dilution 1:2000), p-ERK(Thr^{183} and Tyr^{185}) (dilution 1:5000), PKCα, PKCε, or PKCδ (dilution 1:1000). Following washing, the membranes were incubated with the appropriate secondary antibodies coupled to horseradish peroxidase. Immunocomplexes were visualized with an enhanced chemiluminescence (ECL) detection kit according to the manufacturer's instructions (GE Healthcare, São Paulo, SP, Brazil). Band density measurements were made using the NIH ImageJ 1.36b imaging software (NIH, Bethesda, MD, USA).

2.6. Determination of cytokine levels

Briefly, 6 mm punch-biopsies obtained from the mice ear 24 h after TPA-induced skin inflammation were homogenized in phosphate buffer containing 0.05% Tween 20, 0.1 mM phenylmethylsulphonyl fluoride, 0.1 mM benzethonium chloride, 10 mM EDTA, and 20 IU aprotinin. The homogenate was centrifuged at 3000*g* for 10 min, and supernatants were stored at −70 °C until further

analysis. CXCL1/KC and MIP-2 levels were evaluated using enzyme-linked immunosorbent assay (ELISA) kits from R&D Systems (Minneapolis, MN, USA), according to the manufacturer's recommendations. Protein concentration was determined using the protein assay kit according to the manufacturer's instructions (Bio-Rad, São Paulo, SP, Brazil).

2.7. Assessment of protein kinase C activity

To assess PKC activity, ear samples were homogenized in ice-cold lysis buffer [40 mM Tris-HCl (pH 7,5), 5 mM NaCl, 1 mM $MgCl_2$, 1 mM EDTA, 1 mM phenylmethylsulphonyl fluoride, 10 μg/ml aprotinin, and 10 μg/ml leupeptin], and kept under constant agitation for 45 min at 4 °C. The samples were then centrifuged at 12,000*g* for 60 min at 4 °C, and the supernatant was collected. Protein concentration was determined using the protein assay kit according to the manufacturer's instructions (Bio-Rad, São Paulo, SP, Brazil). PKC activity was analyzed using an ELISA kit according to the manufacturer's instructions (Calbiochem, Darmstadt, Germany).

2.8. Immunohistochemical studies

Ear samples were collected 24 h after TPA-induced skin inflammation and fixed in a PBS solution containing 4% paraformaldehyde for 24 h at room temperature, dehydrated by graded ethanol, and embedded in paraffin. Immunohistochemistry was carried out on paraffin tissue sections (5 μm) using antibodies against vascular endothelial growth factor (VEGF, dilution 1:300) or COX-2 (dilution 1:200). Following quenching of endogenous peroxidase with 1.5% hydrogen peroxide in methanol (v/v) for 20 min, high temperature antigen retrieval was performed by immersion of the slides in a water bath at 95–98 °C in 10 mM trisodium citrate buffer pH 6.0, for 45 min. The slides were then processed using the Vectastain Elite ABC reagent according to the manufacturer's instructions (Vector Laboratories, Burlingame, CA, USA). Following the appropriate biotinylated secondary antibody, sections were developed with DAB in chromogen solution and counterstained with Harris hematoxylin. Control and experimental tissues were placed on the same slide and processed in parallel.

Images of stained skin sections were acquired using a Sight DS-5M-L1 digital camera connected to an Eclipse 50i light microscope (both from Nikon, Melville, NY, USA). Six images per section were captured, and a threshold optical density that best discriminated staining from the background was obtained using the ImageJ 1.36b imaging software. For burden analysis, data were calculated as the labeled area captured (positive pixels) divided by the full area captured (total pixels).

2.9. Statistical analysis

The group Vehicle-Vehicle was considered as control. The percentage of inhibition was calculated over the increase in the response elicited by TPA in the vehicle group (the difference between TPA-Vehicle and Vehicle-Vehicle was considered 100% of response). For Fig. 5, inhibition was calculated as follows: inhibition = {1-([euphol-treated TPA]-[euphol-treated vehicle]/[vehicle-treated TPA]-[vehicle-treated vehicle])} × 100. All the results are presented as mean ± standard error of the mean (SEM). The statistical significance between the groups was assessed by means of one-way , two-way , or repeated-measures ANOVA, followed by the Bonferroni's post-hoc test. The accepted level of significance for the tests was $P < 0.05$.

3. Results

3.1. Effect of euphol on TPA-induced ear edema and cell infiltration

To examine the possible topical antiinflammatory effect of euphol, mice were subjected to a single topical application of TPA in the ear to model skin inflammation. Consistent with previous reports, we observed a rapid onset and time-dependent edematogenic response in TPA-treated mice (Fig. 1a) (De Young et al., 1989). The increase in ear edema was detected after 2 h of TPA treatment, remaining significantly elevated for at least 24 h. Notably, the topical application of euphol (50–100 μg/ear) markedly inhibited the skin inflammation induced by TPA, with both doses significantly affecting ear edema (Fig. 1a). Importantly, the 100 μg/ear dose inhibited the edematogenic response for up to 24 h, and was used in the rest of the experiments. The ear edema induced by TPA was inhibited by 37, 30, 24 and 47% at 4, 6, 12 and 24 h after euphol treatment (100 μg/ear), in that order. In addition, the accumulation of polymorphonuclear and mononuclear cells was also significantly reduced by euphol administration (Fig. 1b and c), as determined by MPO and NAG assays, respectively. The MPO and NAG activities were inhibited by 15 and 42%, respectively, when assessed 24 h after treatment. Administration of euphol to vehicle-treated mice was unable to induce edema or cell infiltration in the mouse ear when compared to control mice (vehicle/vehicle group; data not shown).

In accordance with the MPO assay, topical application of TPA resulted in a significant increase in the levels of the neutrophil chemotactic chemokines CXCL1/KC and MIP-2 when evaluated 24 h after the treatment (Fig. 2). Notably, when mice were treated with euphol (100 μg/ear), the TPA-induced upregulations of CXCL1/KC and MIP-2 were inhibited by 38 and 17%, respectively (Fig. 2A and B).

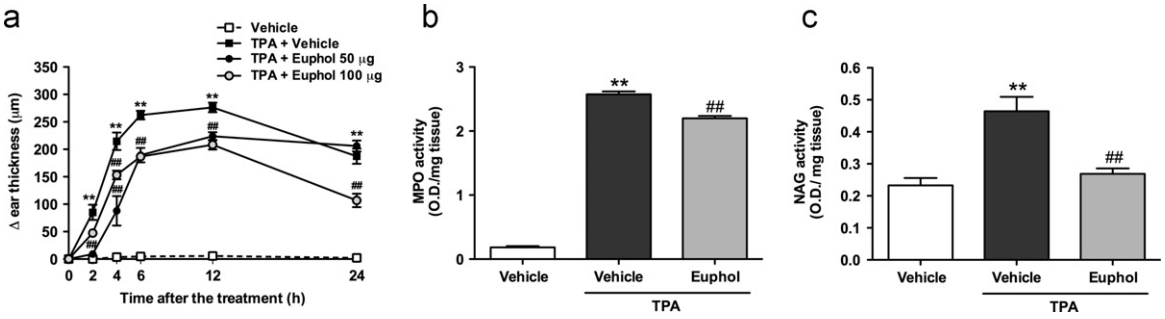

Fig. 1. Effect of euphol on TPA-induced inflammation. Euphol was topically administered (50–100 μg/ear, a; or 100 μg/ear, b and c) in conjunction with TPA. Control animals were treated with vehicle (acetone/ethanol, 3:1). Ear edema (a) was measured at 2, 4, 6, 12, and 24 h after TPA treatment (2.5 μg/ear), and MPO (b) and NAG (c) activities were measured 24 h after TPA treatment. Each point represents the mean ± S.E.M. of 4–7 animals. $^{**}P < 0.01$ compared to vehicle-treated animals. $^{\#\#}P < 0.01$ compared to vehicle/TPA-treated animals. O.D., optical density.

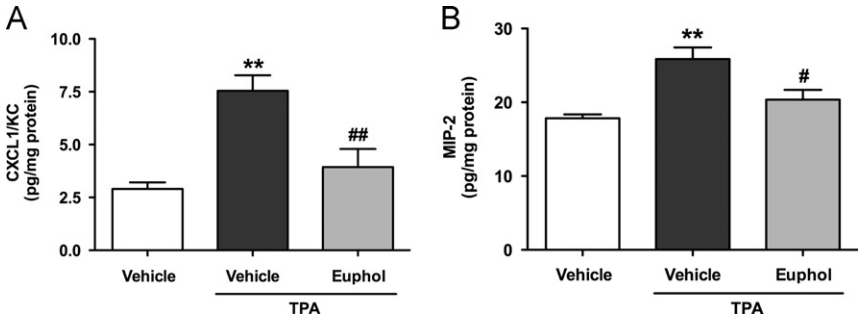

Fig. 2. Euphol administration (100 μg/ear) inhibits TPA-induced chemokine upregulation. (A) CXCL1/KC, and (B) MIP-2 were measured 24 h after TPA treatment (2.5 μg/ear). Each point represents the mean ± S.E.M. of 4–5 animals. $^{**}P < 0.01$ compared to vehicle-treated animals. $^{\#}P < 0.05$ and $^{\#\#}P < 0.01$ compared to vehicle/TPA-treated animals.

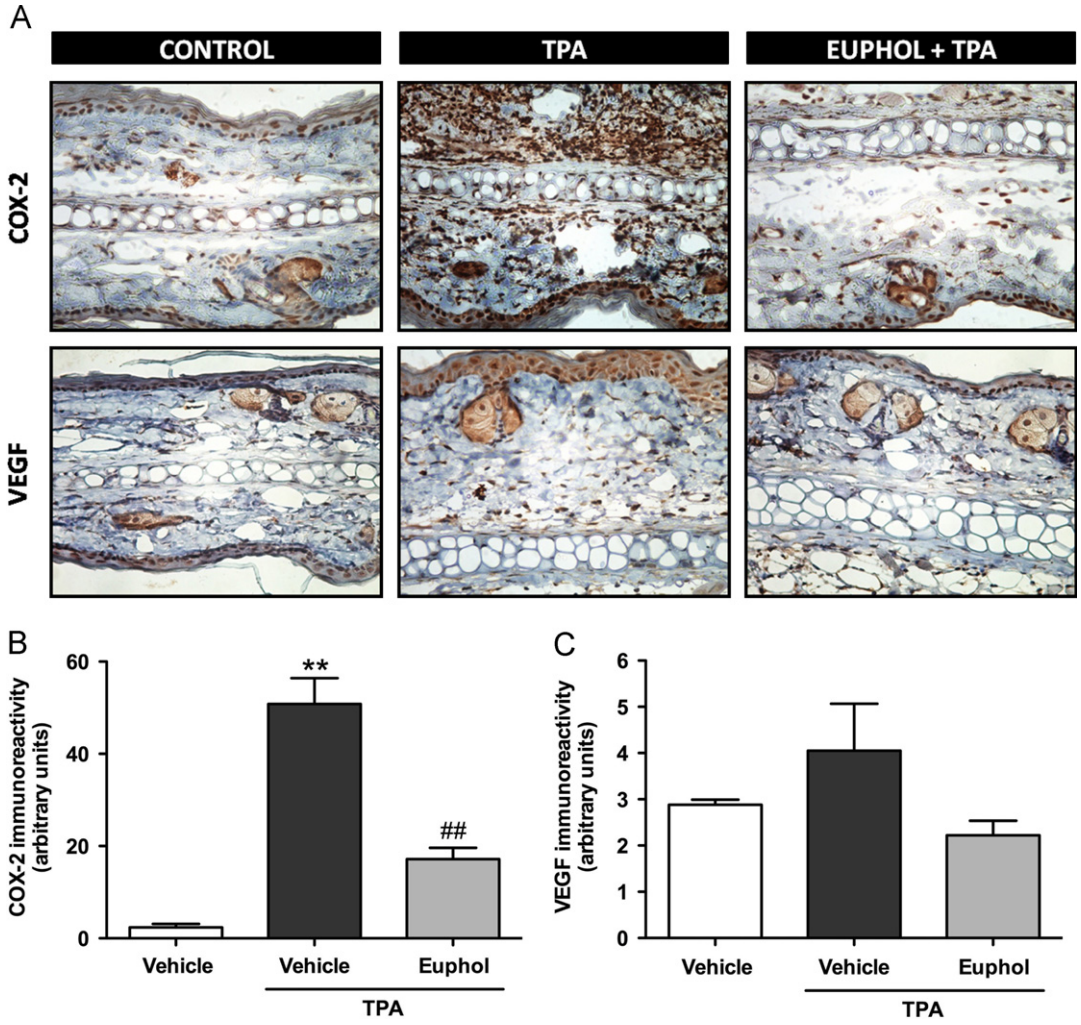

Fig. 3. Euphol administration (100 μg/ear) inhibits TPA-induced COX-2 up-regulation. (A) Representative images, and (B, C) graphic representation of COX-2 and VEGF immunostaining in the mouse ear. Original magnification 400 ×. Immunohistochemical analysis was performed 24 h after TPA treatment (2.5 μg/ear). Each point represents the mean ± S.E.M. of 4–5 animals. $^{**}P < 0.01$ compared to vehicle-treated animals. $^{\#\#}P < 0.01$ compared to vehicle/TPA-treated animals.

3.2. Euphol reduces the TPA-induced COX-2 upregulation

We and others have previously shown that TPA rapidly stimulates COX-2 induction in the mouse skin (Medeiros et al., 2007; Surh et al., 2002). Supporting this data, immunohistochemical analysis revealed that topical application of TPA in the mouse ear resulted in a dramatic (21-fold) upregulation of COX-2 in comparison with vehicle-treated mice when evaluated 24 h after treatment (Fig. 3A and B). In addition, the COX-2 upregulation induced by TPA administration was significantly inhibited (66%) in mice treated with euphol (100 μg/ear). On the other hand, Fig. 3A and C indicate that euphol treatment was incapable of affecting VEGF immunoreactivity in the ear at 24 h after TPA administration.

3.3. Effect of euphol on TPA-induced activation of MAPKs

MAPKs are proteins that mediate the signal transduction from the cell surface to the nucleus, and have been reported as important regulators of inflammatory gene expression in mouse

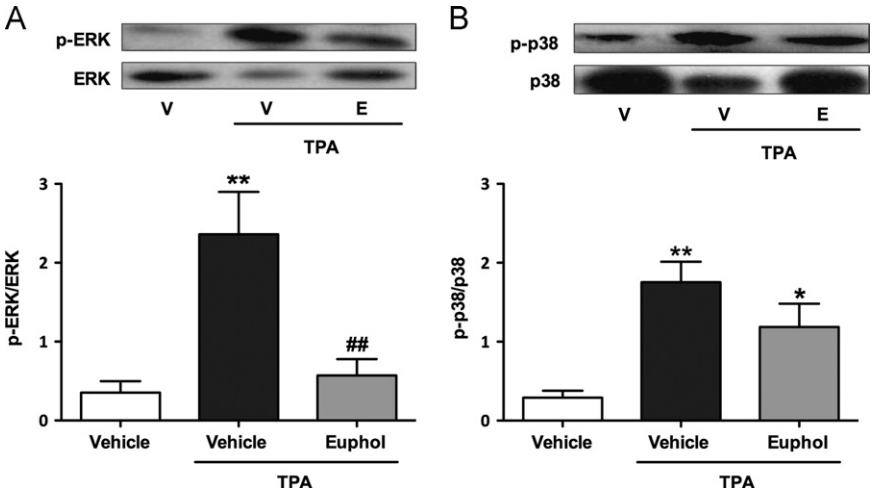

Fig. 4. Effect of euphol (100 μg/ear) on TPA-induced MAPK activation. Western blot analysis of p-ERK (A) and p-p38 MAPK (B) activation was performed 24 h after TPA administration (2.5 μg/ear). Quantification of p-ERK and p-p38 MAPK was normalized by β-actin. Each point represents the mean ± S.E.M. of 4–5 animals. $^{*}P < 0.05$ and $^{**}P < 0.01$ compared to vehicle-treated animals. $^{\#\#}P < 0.01$ compared to vehicle/TPA-treated animals.

skin treated with TPA (Chun et al., 2003). Results of Fig. 4A and B indicate that very low levels of phosphorylated ERK and p38 MAPK are detected under basal conditions in the mouse ear. Conversely, a marked activation of ERK (7-fold; Fig. 4A) and p38 MAPK (6-fold; Fig. 4B) was detected 24 h after the treatment. Of interest, the topical treatment with euphol (100 μg/ear) significantly reduced the TPA-induced activation of ERK by 76%, but not of p38 MAPK (Fig. 4A and B).

3.4. Inhibitory effect of euphol on TPA-induced PKC activation

Phorbol esters, such as TPA, are known to activate a series of PKC iso-enzymes that mediate a strong inflammatory reaction (Mueller, 2006). As expected, data shown in Fig. 5A indicate that topical treatment with TPA resulted in a significant increase in PKC activity in comparison with vehicle-treated mice, when evaluated 2 h after treatment (1.9-fold increase). Moreover, western blot analysis demonstrated that PKCα, PKCδ, and PKCε isoforms were activated by TPA, as shown by increased translocation from cytosol- to membrane-rich fractions (Fig. 5B–D). Notably, the increase in PKC activity induced in the mouse ear by TPA was significantly inhibited by euphol treatment (100 μg/ear) (inhibition of 74%; Fig. 5A). Western blot analysis revealed that euphol prevented activation of PKCα and PKCδ isoforms by 110 and 82%, respectively (Fig. 5B and C). Moreover, TPA-induced PKCε activation was reduced 40% by euphol, although the effect was not significant (Fig. 5D). Of note, administration of euphol to vehicle-treated mice was unable to change PKC activity when compared to control mice (vehicle/vehicle group; Fig. 5).

4. Discussion

In the current study, we demonstrated that topical administration with tetracyclic triterpene euphol, isolated from the sap from *E. tirucalli*, reduces cutaneous inflammation in mice following exposure to the well-characterized protein kinase C activator and tumor promoter TPA. Our data indicate that the mechanisms underlying the antiinflamatory effect of euphol are associated with its ability to prevent edema and leukocyte infiltration, upregulation of COX-2 and chemokines, and activation of ERK, PKCα and PKCδ.

Chronic inflammation has been linked to many steps involved in tumorigenesis, including transformation, promotion, survival, proliferation, invasion, angiogenesis, and metastasis (Aggarwal et al., 2006). In fact, several clinical conditions associated with inflammation appear to predispose the patient to increased susceptibility for skin cancer including lupus erythematosus, dystrophic epidermolysis bullosa, and chronic wound sites (Nickoloff et al., 2005). These observations suggest that antiinflammatory agents may have potential in prevention and treatment of epithelial skin cancers. The topical administration of TPA produces a long-lasting edematogenic response that is associated with a marked influx of mononuclear and polymorphonuclear leukocytes (De Young et al., 1989; Rao et al., 1993). Importantly, our data show that these events are significantly inhibited by euphol administration, as demonstrated by ear thickness, MPO and NAG measurements. MPO is an enzyme found in the azurophilic granules of neutrophils and other cells of myeloid origin, and the utility of its measurement to correlate neutrophil influx is well established (Bradley et al., 1982). Likewise, NAG levels have been used as an indicator of the presence of monocyte/macrophage cells in several inflammatory models (Rao et al., 1993,1994). The recruitment of leukocytes to inflammatory sites is a process largely orchestrated by small polypeptide cytokines known as chemokines (Garin and Proudfoot, 2011). Recently, it was demonstrated that TPA is capable of inducing the upregulation of several chemokines, including the neutrophil chemokines MIP-2 and CXCL1/KC (Cataisson et al., 2006). Corroborating these data, we found significantly increased levels of both chemokines in TPA-treated ears, and topical application of euphol reduced upregulation of MIP-2 and CXCL1/KC, indicating that inhibition of MPO and NAG activities and leukocyte migration in response to TPA may be related to the ability of euphol to inhibit chemokine release.

It is now well recognized that upregulation of COX-2 plays an important role in cancer and chronic inflammation (De Moraes et al., 2007). While COX-2 is usually undetectable in most normal adult tissues including skin, it is highly over expressed in a number of different human cancers, as well as in several animal models of carcinogenesis (Subbaramaiah and Dannenberg, 2003). Importantly, COX-2-selective inhibitors exhibit chemopreventive activity against chemical and ultraviolet light-induced skin carcinogenesis in mice (Chun et al., 2006; Orengo et al., 2002), with genetic ablation of the enzyme resulting in a similar outcome (Fischer et al., 2007; Tiano et al., 2002). In our study, we found a significant inhibitory effect of euphol against TPA-induced COX-2 expression in mouse skin, indicating that the inhibition of TPA-

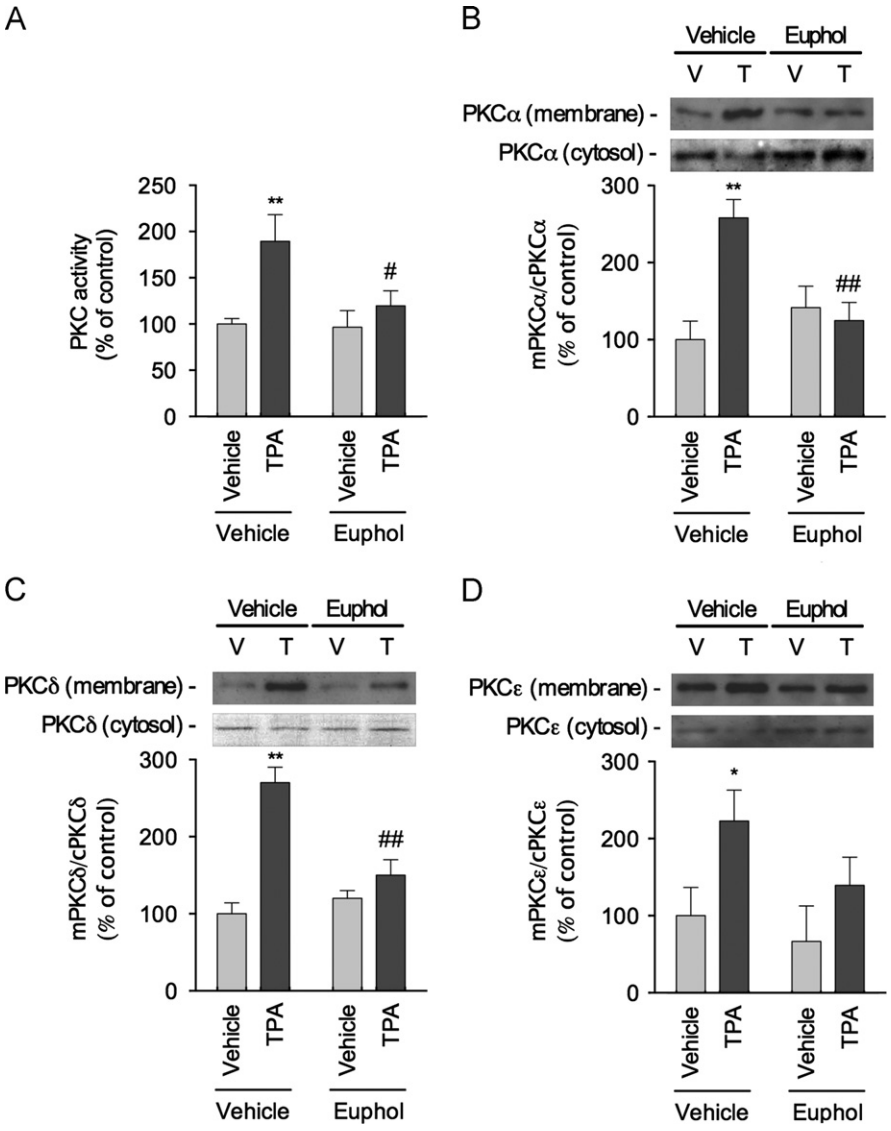

Fig. 5. Effect of euphol (100 μg/ear) on TPA-induced PKC activation. (A) PKC activity on mouse ear protein extracts was analyzed by ELISA 2 h after TPA administration (2.5 μg/ear). (B) PKCα, (C) PKCδ, and (D) PKCε activation was confirmed by western blot analysis of protein translocation from cytosol to membrane. The results represent the ratio of membrane fraction protein detection over that of cytosolic fraction. Each point represents the mean ± S.E.M. of 3–6 animals. $^{*}P < 0.05$ and $^{**}P < 0.01$ compared to vehicle-treated animals. $^{\#}P < 0.05$ and $^{\#\#}P < 0.01$ compared to vehicle/TPA-treated animals.

induced inflammation is in part attributable to the suppression of COX-2 expression.

Next, we evaluated some of the intracellular pathways involved in euphol antiinflammatory effects. The enzymes of the MAP kinase family have been linked to the regulation COX-2 expression and other key proinflammatory genes, including chemokines, and have become one of the most important targets for drug development (Cohen, 2002). In the present study, we demonstrated that topical treatment with euphol greatly inhibited TPA-induced ERK, but not p38 MAPK activation. Of note, several lines of evidence indicate that PKC plays an important role in the activation of the ERK cascade in response to external stimuli, including TPA (Lin et al., 2010).

Protein kinase C comprises a family of serine/threonine kinases first identified as intracellular receptors for tumor-promoting phorbol esters, such as TPA (Kikkawa et al., 1983). These kinases regulate a diverse set of cellular processes including proliferation, apoptosis, cell survival and migration, and there is a substantial amount of evidence linking PKC to tumorigenesis (Griner and Kazanietz, 2007). Notably, PKC activation is significantly reduced in mice treated with euphol, indicating that euphol effects result from a direct action on PKC activity. At present, ten PKC isozymes have been identified and classified in three subfamilies according to the functional domain composition: conventional (cPKCs: PKCα, PKCβI, PKCβII and PKCγ), novel (nPKCs: PKCδ, PKCε, PKCη and PKCθ) and atypical (aPKCs: PKCζ and PKCι) (Mackay and Twelves, 2007). Conventional PKCs are regulated by diacylglycerol (DAG), phosphatidylserine and calcium, whereas novel PKCs are calcium-independent, but regulated by DAG and phosphatidylserine, and atypical PKC isoforms are phosphatidylserine-dependent, but calcium, DAG- and TPA-independent . Since only the former two are activated by TPA, we analyzed the effect of euphol on PKCα, PKCδ, and PKCε activation, the isozymes expressed in human (Fisher et al., 1993) and mouse epidermis (Wang et al., 1993). Interestingly, our data demonstrated that the activation of both PKCα and PKCδ in response to TPA is markedly inhibited by euphol. We also observed a reduction in PKCε activation, although it was not significant. Considerable evidence implicates PKCα in the inflammatory response induced by TPA. Overexpression of PKCα in mouse epidermis exacerbates TPA-induced inflammation

and enhances neutrophil infiltration and the expression of inflammatory proteins including TNF-α, COX-2 and chemokines, an effect dependent on NF-κB activation (Cataisson et al., 2005; Wang and Smart, 1999). Thus, the anti-inflammatory effect of euphol in mouse skin can be related to the direct inhibition of PKCα, resulting in reduced expression of COX-2, MIP-2 and CXCL1/KC.

The isozymes of PKC family have been shown to exhibit distinct roles in induction of skin cancer (Aziz et al., 2007). Notably, PKCδ and PKCε transgenic mice show different responses to skin tumor promotion by TPA, with PKCε overexpressing transgenic mice exhibiting enhanced carcinoma elicited by the two-step DMBA-TPA protocol (Reddig et al., 2000), while increased expression of PKCδ in the mouse epidermis suppresses the formation of carcinomas (Reddig et al., 1999). Considering the opposing roles of PKCδ and PKCε in cancer, additional studies are necessary to further characterize the effect of euphol in these isozymes.

5. Conclusion

In the present data, we have provided in vivo evidence that the plant-derived tetracyclic triterpene euphol exhibits strong topical anti-inflammatory actions on mouse ear inflammation induced by TPA, through a mechanism that involves its ability to regulate PKC and ERK activation, resulting in reduced COX-2, MIP-2 and CXCL1/KC upregulation and leukocyte infiltration. Taken together, our data suggests that euphol may be a good candidate for the treatment of skin disorders with an inflammatory component, including cancer, although additional experiments using chronic models need to be conducted to further establish the potential efficacy of euphol in these conditions.

Acknowledgments

This work was supported by Grants from Amazônia Fitomedicamentos, Brazil, the Conselho Nacional de Desenvolvimento Científico e Tecnológico (CNPq), the Coordenação de Aperfeiçoamento de Pessoal de Nível Superior (CAPES), the Programa de Apoio aos Núcleos de Excelência (PRONEX), and the Fundação de Apoio à Pesquisa do Estado de Santa Catarina (FAPESC).

References

Aggarwal, B.B., Shishodia, S., Sandur, S.K., Pandey, M.K., Sethi, G., 2006. Inflammation and cancer: how hot is the link? Biochem. Pharmacol. 72, 1605–1621.

Aziz, M.H., Manoharan, H.T., Sand, J.M., Verma, A.K., 2007. Protein kinase Cepsilon interacts with Stat3 and regulates its activation that is essential for the development of skin cancer. Mol. Carcinog. 46, 646–653.

Bickers, D.R., Athar, M., 2006. Oxidative stress in the pathogenesis of skin disease. J. Invest. Dermatol. 126, 2565–2575.

Bradley, P.P., Priebat, D.A., Christensen, R.D., Rothstein, G., 1982. Measurement of cutaneous inflammation: estimation of neutrophil content with an enzyme marker. J. Invest. Dermatol. 78, 206–209.

Cataisson, C., Pearson, A.J., Torgerson, S., Nedospasov, S.A., Yuspa, S.H., 2005. Protein kinase C alpha-mediated chemotaxis of neutrophils requires NF-kappa B activity but is independent of TNF alpha signaling in mouse skin in vivo. J. Immunol. 174, 1686–1692.

Cataisson, C., Pearson, A.J., Tsien, M.Z., Mascia, F., Gao, J.L., Pastore, S., Yuspa, S.H., 2006. CXCR2 ligands and G-CSF mediate PKCalpha-induced intraepidermal inflammation. J. Clin. Invest. 116, 2757–2766.

Chun, K.S., Keum, Y.S., Han, S.S., Song, Y.S., Kim, S.H., Surh, Y.J., 2003. Curcumin inhibits phorbol ester-induced expression of cyclooxygenase-2 in mouse skin through suppression of extracellular signal-regulated kinase activity and NF-kappa B activation. Carcinogenesis 24, 1515–1524.

Chun, K.S., Kundu, J.K., Park, K.K., Chung, W.Y., Surh, Y.J., 2006. Inhibition of phorbol ester-induced mouse skin tumor promotion and COX-2 expression by celecoxib: C/EBP as a potential molecular target. Cancer Res. Treat. 38, 152–158.

Cohen, P., 2002. Protein kinases–the major drug targets of the twenty-first century? Nat. Rev. Drug Discov. 1, 309–315.

De Melo, J.G., Santos, A.G., De Amorim, E.L., Do Nascimento, S.C., De Albuquerque, U.P., 2011. Medicinal plants used as antitumor agents in Brazil: an ethnobotanical approach. Evid. Based Complement Altern. Med., 365359.

De Moraes, E., Dar, N.A., de Moura Gallo, C.V., Hainaut, P., 2007. Cross-talks between cyclooxygenase-2 and tumor suppressor protein p53: Balancing life and death during inflammatory stress and carcinogenesis. Int. J. Cancer 121, 929–937.

De Young, L.M., Kheifets, J.B., Ballaron, S.J., Young, J.M., 1989. Edema and cell infiltration in the phorbol ester-treated mouse ear are temporally separate and can be differentially modulated by pharmacologic agents. Agents Actions 26, 335–341.

Dutra, R.C., de Souza, P.R., Bento, A.F., Marcon, R., Bicca, M.A., Pianowski, L.F., Calixto, J.B., 2012. Euphol prevents experimental autoimmune encephalomyelitis in mice: evidence for the underlying mechanisms. Biochem. Pharmacol. 83, 531–542.

Fischer, S.M., Pavone, A., Mikulec, C., Langenbach, R., Rundhaug, J.E., 2007. Cyclooxygenase-2 expression is critical for chronic UV-induced murine skin carcinogenesis. Mol. Carcinog. 46, 363–371.

Fisher, G.J., Tavakkol, A., Leach, K., Burns, D., Basta, P., Loomis, C., Griffiths, C.E., Cooper, K.D., Reynolds, N.J., Elder, J.T., et al., 1993. Differential expression of protein kinase C isoenzymes in normal and psoriatic adult human skin: reduced expression of protein kinase C-beta II in psoriasis. J. Invest. Dermatol. 101, 553–559.

Garin, A., Proudfoot, A.E., 2011. Chemokines as targets for therapy. Exp. Cell. Res. 317, 602–612.

Griner, E.M., Kazanietz, M.G., 2007. Protein kinase C and other diacylglycerol effectors in cancer. Nat. Rev. Cancer 7, 281–294.

Hvid, H., Teige, I., Kvist, P.H., Svensson, L., Kemp, K., 2008. TPA induction leads to a Th17-like response in transgenic K14/VEGF mice: a novel in vivo screening model of psoriasis. Int. Immunol. 20, 1097–1106.

Johnson-Huang, L.M., McNutt, N.S., Krueger, J.G., Lowes, M.A., 2009. Cytokine-producing dendritic cells in the pathogenesis of inflammatory skin diseases. J. Clin. Immunol. 29, 247–256.

Kikkawa, U., Takai, Y., Tanaka, Y., Miyake, R., Nishizuka, Y., 1983. Protein kinase C as a possible receptor protein of tumor-promoting phorbol esters. J. Biol. Chem. 258, 11442–11445.

Levy, J.H., 1996. The human inflammatory response. J. Cardiovasc. Pharmacol. 27 (1), S31–37.

Lin, C.W., Shen, S.C., Chien, C.C., Yang, L.Y., Shia, L.T., Chen, Y.C., 2010. 12-O-tetradecanoylphorbol-13-acetate-induced invasion/migration of glioblastoma cells through activating PKCalpha/ERK/NF-kappaB-dependent MMP-9 expression. J. Cell Physiol. 225, 472–481.

Mackay, H.J., Twelves, C.J., 2007. Targeting the protein kinase C family: are we there yet? Nat. Rev. Cancer 7, 554–562.

Medeiros, R., Otuki, M.F., Avellar, M.C., Calixto, J.B., 2007. Mechanisms underlying the inhibitory actions of the pentacyclic triterpene alpha-amyrin in the mouse skin inflammation induced by phorbol ester 12-O-tetradecanoylphorbol-13-acetate. Eur. J. Pharmacol 559, 227–235.

Mueller, M.M., 2006. Inflammation in epithelial skin tumours: old stories and new ideas. Eur. J. Cancer 42, 735–744.

Nickoloff, B.J., Ben-Neriah, Y., Pikarsky, E., 2005. Inflammation and cancer: is the link as simple as we think? J Invest Dermatol 124, 10–14 .

Orengo, I.F., Gerguis, J., Phillips, R., Guevara, A., Lewis, A.T., Black, H.S., 2002. Celecoxib, a cyclooxygenase 2 inhibitor as a potential chemopreventive to UV-induced skin cancer: a study in the hairless mouse model. Arch. Dermatol. 138, 751–755.

Otuki, M.F., Vieira-Lima, F., Malheiros, A., Yunes, R.A., Calixto, J.B., 2005. Topical antiinflammatory effects of the ether extract from Protium kleinii and alpha-amyrin pentacyclic triterpene. Eur. J. Pharmacol. 507, 253–259.

Rao, T.S., Currie, J.L., Shaffer, A.F., Isakson, P.C., 1993. Comparative evaluation of arachidonic acid (AA)- and tetradecanoylphorbol acetate (TPA)-induced dermal inflammation. Inflammation 17, 723–741.

Rao, T.S., Shaffer, A.F., Currie, J.L., Isakson, P.C., 1994. Role of mast cells in calcium ionophore (A23187)-induced peritoneal inflammation in mice. Inflammation 18, 187–192.

Reddig, P.J., Dreckschmidt, N.E., Ahrens, H., Simsiman, R., Tseng, C.P., Zou, J., Oberley, T.D., Verma, A.K., 1999. Transgenic mice overexpressing protein kinase Cdelta in the epidermis are resistant to skin tumor promotion by 12-O-tetradecanoylphorbol-13-acetate. Cancer Res. 59, 5710–5718.

Reddig, P.J., Dreckschmidt, N.E., Zou, J., Bourguignon, S.E., Oberley, T.D., Verma, A.K., 2000. Transgenic mice overexpressing protein kinase C epsilon in their epidermis exhibit reduced papilloma burden but enhanced carcinoma formation after tumor promotion. Cancer Res. 60, 595–602.

Robert, C., Kupper, T.S., 1999. Inflammatory skin diseases, T cells, and immune surveillance. N. Engl. J. Med. 341, 1817–1828.

Subbaramaiah, K., Dannenberg, A.J., 2003. Cyclooxygenase 2: a molecular target for cancer prevention and treatment. Trends Pharmacol. Sci. 24, 96–102.

Surh, Y.J., Lee, J.Y., Choi, K.J., Ko, S.R., 2002. Effects of selected ginsenosides on phorbol ester-induced expression of cyclooxygenase-2 and activation of NF-kappaB and ERK1/2 in mouse skin. Ann. NY Acad. Sci. 973, 396–401.

Tiano, H.F., Loftin, C.D., Akunda, J., Lee, C.A., Spalding, J., Sessoms, A., Dunson, D.B., Rogan, E.G., Morham, S.G., Smart, R.C., Langenbach, R., 2002. Deficiency of either cyclooxygenase (COX)-1 or COX-2 alters epidermal differentiation and reduces mouse skin tumorigenesis. Cancer Res. 62, 3395–3401.

Valadares, M.C., Carrucha, S.G., Accorsi, W., Queiroz, M.L., 2006. *Euphorbia tirucalli* L. modulates myelopoiesis and enhances the resistance of tumour-bearing mice. Int. Immunopharmacol. 6, 294–299.

Verma, A.K., Wheeler, D.L., Aziz, M.H., Manoharan, H., 2006. Protein kinase Cepsilon and development of squamous cell carcinoma, the nonmelanoma human skin cancer. Mol. Carcinog. 45, 381–388.

Wang, H.Q., Smart, R.C., 1999. Overexpression of protein kinase C-alpha in the epidermis of transgenic mice results in striking alterations in phorbol ester-induced inflammation and COX-2, MIP-2 and TNF-alpha expression but not tumor promotion. J. Cell Sci. 112, 3497–3506.

Wang, X.J., Warren, B.S., Beltran, L.M., Fosmire, S.P., DiGiovanni, J., 1993. Further identification of protein kinase C isozymes in mouse epidermis. J. Cancer Res. Clin. Oncol. 119, 279–287.

Yasukawa, K., Akihisa, T., Yoshida, Z.Y., Takido, M., 2000. Inhibitory effect of euphol, a triterpene alcohol from the roots of *Euphorbia kansui*, on tumour promotion by 12-O-tetradecanoylphorbol-13-acetate in two-stage carcinogenesis in mouse skin. J. Pharm. Pharmacol. 52, 119–124.